Electronic Supplementary Material (ESI) for New Journal of Chemistry.

Electronic Supporting Information for:

Boronic Acids for Functionalisation of Commercial Multi-Layer Graphitic Material as an Alternative to Diazonium Salts

Rachel L. McLaren, Christian J. Laycock, David J. Morgan, and Gareth R. Owen*

Table of Contents

A. Additional XPS data

As outlined within the manuscript, XPS analysis revealed the presence of nitrogen Again, some nitrogen species within the MLG, ^{Ar}*f*-MLG and ^{c}*Ox*-MLG materials at atomic % of 0.32%, 0.26% and 0.20%. These are impurities which are present within the source material. As shown in Figure S1, below the spectra were not sufficiently clear to provide any insight into the nature of the nitrogen based functional groups present.

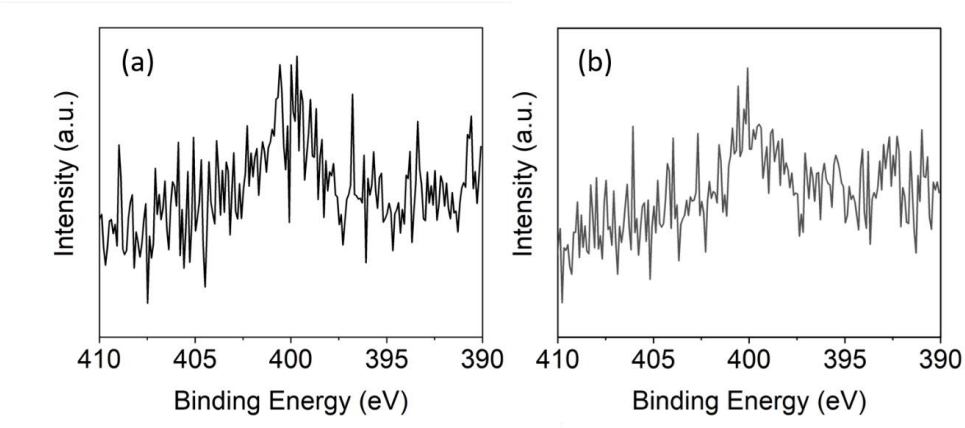

Figure S1 – XPS spectra for N 1s orbital for MLG (a) and ^{Ar}*f*-MLG (b)

B. Raman Spectroscopy

Raman spectroscopy was used to examine the structure of ^{c}*Ox*-MLG as outlined in the manuscript (Figure S3). This exhibited changes with respect to the starting MLG. The I_D/I_G and I_{2D}/I_G ratios were found to be 0.56 and 0.40 (*c.f.* with the values 0.65 and 0.47 for ^{Ar}*f*-MLG).

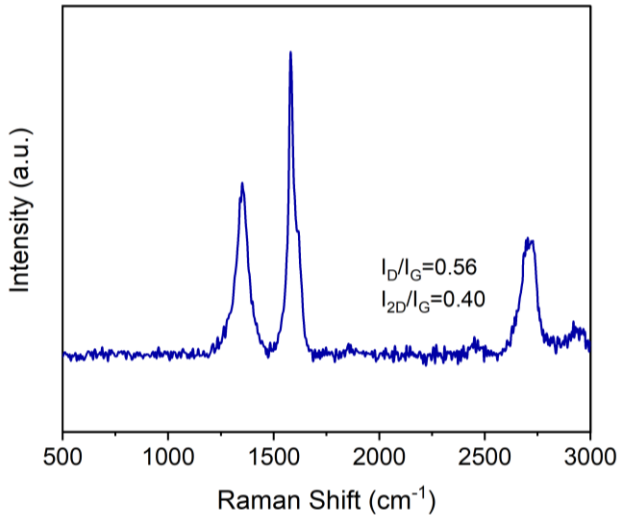

Figure S2 –Raman spectra for ^{C}*Ox*-MLG

C. Further details and discussion on X-ray Diffraction Studies

Analysis of the 2θ = 26° signal

The combination of hexagonal (2H) and rhombohedral (3H) phases to the peak around 2θ = 26° corresponding to the (002)/(003) graphitic peak can be utilised to calculate the *out of plane crystallite size*, $\boldsymbol{L_c}$ the *in-plane crystallite size*, $\boldsymbol{L_a}$, the number of graphene layers, $\boldsymbol{N_c}$ and the interlayer spacing, $\boldsymbol{d_{(002)/(003)}}$ for graphitic stacks. This can be achieved using the Scherrer equation and Bragg's equations shown below. Within these equations, **K** corresponds to the shape factor which takes values of 0.91 and 1.84, for equations corresponding to $\mathbf{L_c}$ and $\mathbf{L_a}$ respectively. The value **λ** corresponds to CuK_α radiation (0.154185 nm), **θ** corresponds to the Bragg angle, **β** corresponds to the full width at half maximum (FWHM) and n corresponds to the order of diffraction. The **β** values were determined by Gaussian and Lorentz fitting of the $\boldsymbol{d_{(002)/(003)}}$ peak within MLG and ^{Ar}*f*-MLG using *OriginPro* software. These are shown in Figure S1 below.

$$L_c = \frac{K\lambda}{\beta \cos\theta} \qquad \textbf{Equation 1} \textit{ Scherrer equation for out-plane crystallite size (K = 0.91)}$$

$$L_a = \frac{K\lambda}{\beta \cos\theta} \qquad \textbf{Equation 2} \textit{ Scherrer equation for in-plane crystallite size (K = 1.84)}$$

$$N_c = \frac{L_c}{d_{\frac{002}{003}}} \qquad \textbf{Equation 3} \textit{ Calculation for the number of graphene layers}$$

$$2d_{\frac{002}{003}} \sin\theta = n\lambda \qquad \textbf{Equation 4 Bragg Equation}$$

The FWHM (**β**) is calculated for both materials, using *OriginPro* software, using Gaussian and Lorentz fitting. Note: Within OriginPro the FWHM is denoted as "**w**" in degrees. It was found that the Lorentz fit was better for MLG. The fits were similar for ^{Ar}*f*-MLG.

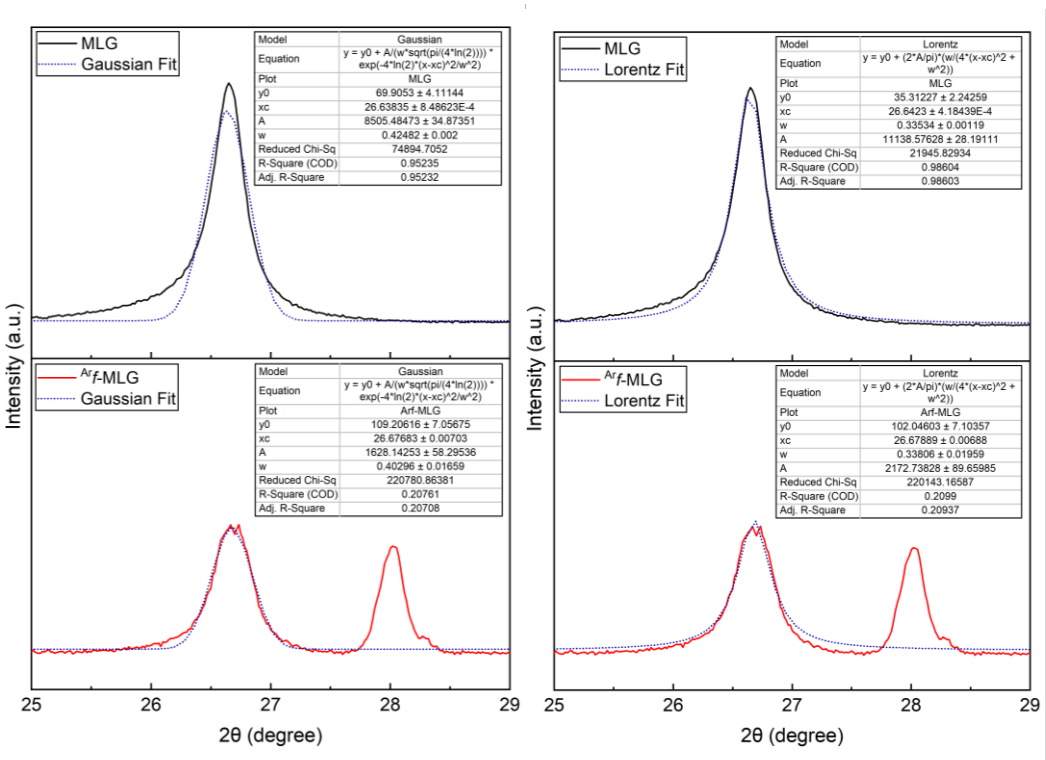

Figure S3 – Gaussian and Lorentz fitting of the $d_{(002)/(003)}$ peak within MLG (top) and ^{Ar}*f*-MLG (bottom) to gain FWHM values, carried out using OriginPro software. The line at approximately 28° is associated with the presence of silver as outlined within the main article

Table S1 – Calculated values of $\mathbf{L_c}$, $\mathbf{L_a}$, $\mathbf{N_c}$ and $\mathbf{d_{(002)/(003)}}$ using Equations 1 – 4

	Material	Interlayer Spacing (*d*) (nm)	FWHM (radians)	Crystallite size, L_c(nm)	In-Plane Crystallite Size, L_a(nm)	Number of graphene layers (L_c)/d(002)
Gaussian Model	MLG	0.334349886	0.42482	19.42952	39.28607	58.11135349
	^{Ar}f-MLG	0.333869932	0.40295	20.48571	41.42165	61.35835037
Lorentz Model	MLG	0.334300595	0.33534	24.61418	49.76933	73.62888182
	^{Ar}f-MLG	0.333845357	0.33806	24.418	49.37267	73.14166006

Determination of the ratio of 2H:3R phases within MLG

The ratio of 2H:3R phases within MLG was calculated according to the ratio of the 3R (101) to 2H (101) peaks. Figure S2 depicts a deconvoluted spectra of the overlapping four lined pattern consisting of the 2H (100), 3R (101), 2H (101) and 3R (012) phases. Gaussian fitting of the peaks reveals the corresponding areas associated with each peak. The integrated ratio of 3R (101) to 2H (101) corresponds to 658.045:688.167 (48.88/51.12%). This ratio is not dissimilar to those values obtained by Seehra and co-workers when examining a range of commercially synthesised multilayer graphenes.[R1] The 3R (101) to 2H (101) could not be deconvoluted for ^{Ar}f-MLG since the 2H (101) peak overlaps with that of a Ag reflection, and the peaks were too low intensity. Whilst the models give different FWHM values, and therefore stacking numbers, they appear similar for MLG and ^{Ar}f-MLG in both cases, suggesting there is little change to the crystallite size and stacks numbers within the crystallites.

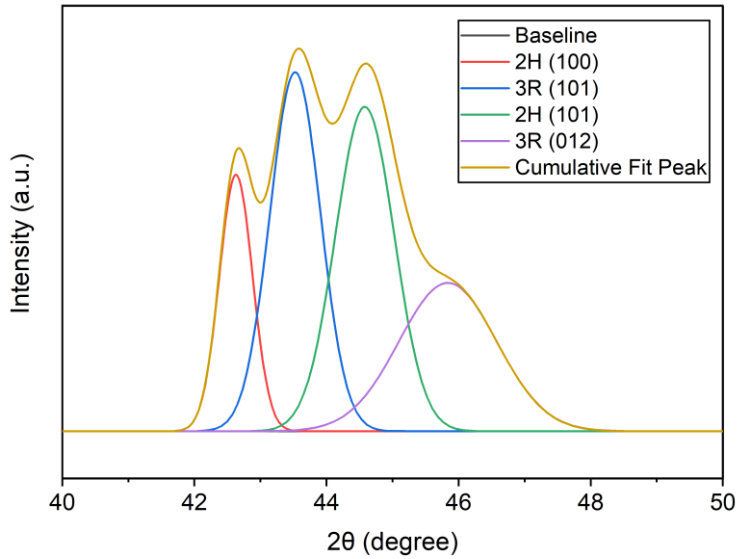

Figure S4 – Gaussian fitting of the four lined pattern associated with the 2H (100), 3R (101), 2H (101) and 3R (012) phases and the corresponding data as provided by OriginPro software.

Table S2 – Gaussian Fitted values of the deconvolution of the four lined pattern associated with the 2H (100), 3R (101), 2H (101) and 3R (012) phases

Peak Index	Peak Type	Area Intg	FWHM	Max Height	Center Grvty	Area IntgP
2H (100)	Gaussian	308.88756	0.59406	488.46971	42.62814	14.1802
3R (101)	Gaussian	658.04454	0.90418	683.70256	43.52429	30.20906
2H (101)	Gaussian	688.16695	1.04648	617.77677	44.57866	31.5919
3R (012)	Gaussian	523.20313	1.7396	282.5457	45.83542	24.01885

R1 M. S. Seehra, U. K. Geddam, D. Schwegler-Berry and A. B. Stefaniak, Carbon N. Y., 2015, **95**, 818–823.

D. Additional SEM Images

Additional SEM images are provided below to highlight the various structural features found within the ^{Ar}f-MLG material. Figure S5 highlights the stacking within the material. Figure S6 shows a closer perspective of the bottom right hand corner of Figure S5 which see two stacks partially separated. There are a number of smaller flakes and particles on these surfaces. Figure S7 shows both ^{Ar}f-MLG flakes on the left of the picture and silver nanoparticles as spherical structures on the right and the bottom.

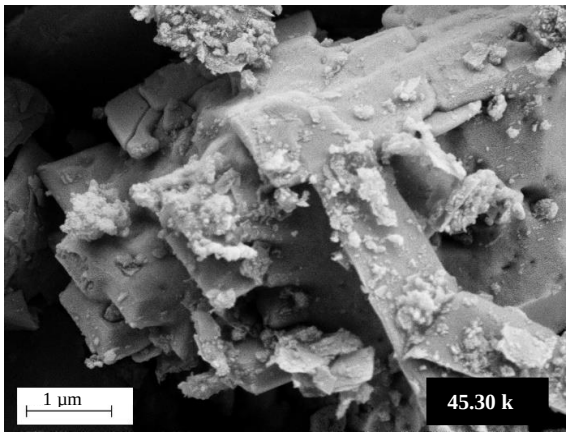

Figure S5 – ^{Ar}f-MLG flakes at a magnification of 45,300 x

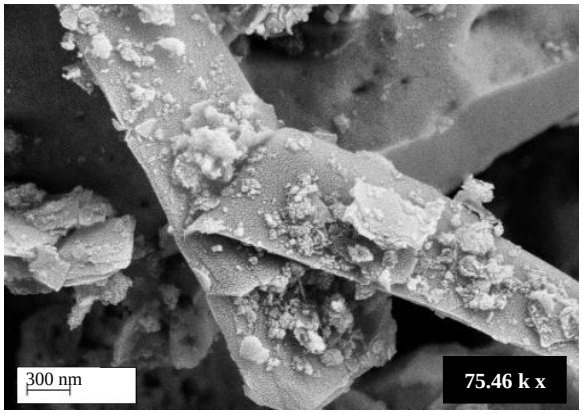

Figure S6 – ^{Ar}f-MLG flakes at a magnification of 75,460 x

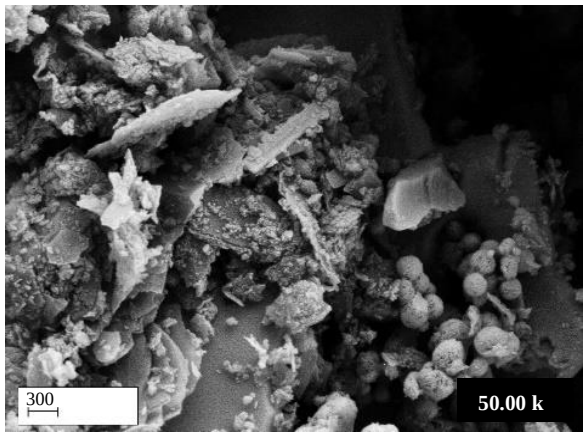

Figure S7 – ^{Ar}f-MLG flakes and silver nanoparticles